Distinguishing remobilized ash from erupted volcanic plumes using space-borne multi-angle imaging.

Verity J. B. Flower[1,2] and Ralph A. Kahn[1]

[1]Climate and Radiation Laboratory, Earth Science Division, NASA Goddard Space Flight Center, Greenbelt, MD 20771, USA

[2]Universities Space Research Association, 7178 Columbia Gateway Drive, Columbia, MD 21046, USA

Corresponding author – verity.j.flower@nasa.gov

Abstract

Volcanic systems are comprised of a complex combination of ongoing eruptive activity and secondary hazards, such as remobilized ash plumes. Similarities in the visual characteristics of remobilized and erupted plumes, as imaged by satellite-based remote sensing, complicate the accurate classification of these events. The stereo imaging capabilities of the Multi-angle Imaging SpectroRadiometer (MISR) were used to determine the altitude and distribution of suspended particles. Remobilized ash shows distinct dispersion, with particles distributed within ~1.5 km of the surface. Particle transport is consistently constrained by local topography, limiting dispersion pathways downwind. The MISR Research Aerosol (RA) retrieval algorithm was used to assess plume particle microphysical properties. Remobilized ash plumes displayed a dominance of large particles with consistent absorption and angularity properties, distinct from emitted plumes. The combination of vertical distribution, topographic control, and particle microphysical properties makes it possible to distinguish remobilized ash flows from eruptive plumes, globally.

Keywords – Remobilized ash; volcanic plumes; remote sensing; MISR; Kamchatka.

1. Introduction

Volcanic eruptions produce a variety of hazards, broadly defined as primary, generated by eruptive events, and secondary, generated by the interaction of previously erupted volcanic products with external forces. Common secondary volcanic hazards include lahars (volcanic mudflows) and remobilized volcanic ash plumes (particles re-suspended by high winds). The identification of remobilized ash plumes with satellite imaging can be complicated by their visual

similarity to erupted emissions (Flower & Kahn, 2017). Incomplete records limit studies on remobilized plumes. The misclassification of these secondary hazards can also falsely inflate the volcano eruptive statistics (Flower & Kahn, 2017), particularly where minimal ground-based monitoring is available for classification purposes. To conduct an in-depth analysis of remobilized ash events, a method for distinguishing these plumes from active eruptions is required. Particles re-suspended into the boundary layer by strong winds should display characteristics distinct from erupted plumes due to differences in the plume generation processes. For example, we expect the vertical profiles of suspended particles, and possibly also particle property differences, to help distinguish erupted plumes from remobilized ash.

Multi-angle imaging obtained by NASA's Multi-angle Imaging SpectroRadiometer (MISR) provides constraints on airborne particle vertical distribution. The ~380 km swath of MISR, maintained in polar Low Earth Orbit (LEO), produces revisit timing ranging from 8 days at the equator to 2 days near the poles. The increased revisit time in high latitude regions, due to orbital track convergence, makes monitoring of Kamchatka, Russia ideal. Kamchatka hosts multiple active volcanoes within the MISR mission period (2000-present), located between 51°N and 57°N latitude. A review of all coincident MISR orbits, using the methodology as described in Flower & Kahn (2017), identified 115 plumes from eight volcanoes during this period: Shiveluch, Kliuchevskoi, Bezymianny, Tolbachik, Kizimen, Karymsky, Zhupanovsky and Kambalny. A distinct subgroup of 19 plumes display characteristics similar to those expected from remobilized ash. These plumes were observed most frequently from July through early November (Flower & Kahn, 2017).

The remainder of this paper details the unique features of remobilized ash plumes, as distinct from eruptive plumes, in the MISR imagery.

2. Methodology

MISR flies aboard NASA's Terra satellite, launched in December 1999, providing over 17-years of near-global observations. MISR observes in four spectral bands, at 446, 558, 672 and 866 nm. It is unique in providing near-coincident imagery from nine cameras that view the surface at nadir, plus four steeper angles (26.1°, 45.6°, 60°, 70.5°), in the forward (F) and aft (A) directions (Diner et al., 1998). MISR data are provided at 1.1 km resolution, with improved resolution (275 m) available at nadir and in the red spectral band at all other angles. The varying view angles provide details of particle suspension altitude (Moroney et al., 2002; Muller et al., 2002; Kahn et

al., 2007; Scollo et al., 2010; Nelson et al., 2008; 2013), and the range scattering angles and atmospheric path lengths contain information about particle amount and microphysical properties (Kahn & Limbacher 2012; Kahn & Gaitley 2015; Limbacher & Kahn 2014; 2017). As comprehensive assessment of particle property retrieval quality over land is currently limited, microphysical properties presented here include only those sections of plumes extending over dark water off the Kamchatka coast (Supplemental Material; 12 remobilized; 19 erupted).

2.1. MISR plume profiling

Plume height is derived from the parallax observed by matching MISR stereo images of plumes (Nelson et al., 2008; 2013). Parallax is the apparent shift in the position of visible atmospheric features relative to the underlying surface in different angular views. In practical terms, low-altitude plumes display minimal parallax, whereas higher-altitude features appear to move progressively more (Figure 1). The MISR INteractive eXplorer (MINX) (Nelson et al., 2008; 2013) is a software package that derives plume elevations from MISR hyper-stereo imagery, and was used here to map plume vertical extent. Users are required to outline the plume area and indicate the wind direction, from which elevations are retrieved at 1.1 km horizontal resolution; vertical resolution ranges from ~250 to 500 m, depending on retrieval conditions and whether the blue or higher-horizontal-resolution red band imagery is used (Nelson et al., 2013). Corrections are made to account for plume proper motion between the times different cameras observe a given surface location (<7 min). The retrievals actually determine the elevation of maximum spatial contrast for each pixel, and because most aerosol plumes are not uniform, the aggregated vertical distribution of retrieved pixel heights gives some indication of the aerosol layer vertical profile. Although red band (672 nm) retrievals have the best horizontal spatial resolution, successful height retrievals can be limited when contrast with the surface is low, e.g., over land, especially when plume aerosol optical depth (AOD) is low. Where few red band retrievals are successful, the blue band (446 nm) is used, as AOD tends to be higher at this wavelength. Plume heights are retrieved as Above Sea Level (ASL), with the corresponding terrain elevation also identified on height distribution plots (Fig. 2; Supplemental Material). A lower limit for plume retrieval height was set within MINX to 250 m above terrain height, reducing the risk of contamination by surface signals. As such, wind-corrected plume heights for particles below 250 m are not retrieved or displayed in the MINX plots presented here. MISR-derived volcanic plume heights have previously been found to display consistency with traditional observations (e.g., Scollo et al., 2012; Flower & Kahn, 2017).

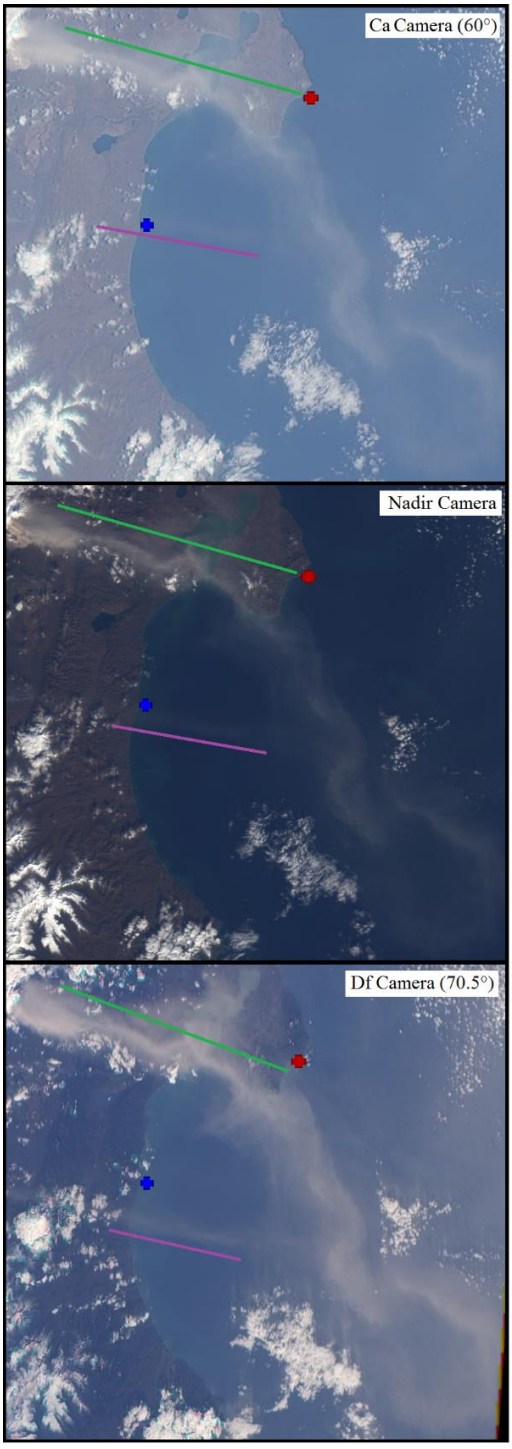

Figure 1 – MISR images obtained on October 4, 2016 from: the 60° aft-viewing camera (Ca); the nadir camera; and the 70.5° forward-viewing camera (Df). Lines indicate the upper edge of the remobilized plume from Shiveluch (green) and the lower edge of the erupted plume from Kliuchevskoi (purple). Red and blue dots highlight fixed points in the images based on distinct coastal landmarks. Comparing plume line and dot positions indicates the apparent shift in plume position, relative to ground features. (Terra Orbit: 89366; Path: 98; MISR Blocks: 45-47)

2.2. Plume microphysical properties

The microphysical properties of suspended particles are difficult to categorize *in situ*, due to the innate hazards associated with direct sampling. Alternative techniques include collecting particles deposited on the surface, and remote-sensing methods. The sampling of deposited particles can provide skewed results, as sorting and aggregation can occur during the settling process. Remote sensing methods hold the potential to retrieve information about plume particles in suspension. However, relating optical properties derived from remote sensing to physical and chemical properties is not straightforward, especially for volcanic ash. Particle optical models are commonly assumed, based on laboratory analysis of surface samples. The limited number of volcanic plume measurements, and the varying properties of emitted particles, even from the same eruption of the same volcano, complicates the development of specific volcanic particle optical models. The MISR Standard Aerosol (SA; Martonchik.et al., 2002; 2009) and Research Aerosol (RA; Kahn et al., 2001; Limbacher & Kahn 2014) retrieval algorithms derive particle properties by comparing observed radiances against those simulated for aerosol mixtures with predetermined optical properties. Particles with different optical properties produce variations in the observed multi-angle, multi-spectral radiance signatures. This approach has been used to retrieve particle-type constraints for dust (Kalashnikova et al., 2005; Kalashnikova & Kahn, 2006; 2008), volcanic plumes (Kahn & Limbacher 2012; Scollo et al. 2012) and global aerosol typing (Kahn & Gaitley, 2015). For volcanic plumes in particular, the MISR radiance signature of ash particles has been approximated by different mixtures of large, non-spherical, non-absorbing "cirrus" and slightly absorbing "dust grain" optical analogs, combined with large spherical non-absorbing and small spherical absorbing particles (Kahn & Limbacher 2012). The SA runs with 74 pre-determined mixtures comprised of up to three of eight individual aerosol components (Kahn et al., 2010), whereas for the current study, the RA classified observed radiances using 774 mixtures comprised of up to three of 14 components (Limbacher & Kahn, 2014; 2017).

Despite the limitations previously discussed, comparison of RA mixture analogs reveals qualitative differences in physical properties of emissions across and between plumes. Scollo et al. (2012) used the fraction of spherical particles in SA retrievals to distinguish SO_2-dominant from ash-dominant plumes from Mount Etna, and validated the results against extensive ground-based records. As in previous work, we interpret the RA output in terms of the fraction of mid-visible AOD assigned to broad particle property classes: size (small - < 0.2 μm, medium – 0.2 – 1 μm, large - > 1 μm), shape (spherical, spheroid, non-spherical), and light absorption or Single

Scattering Albedo (SSA) (strongly absorbing - 0.8, mildly absorbing - 0.9, non-absorbing - 1.0) within each MISR-imaged plume.

3. Distinguishing plume types

3.1. Plume height distributions

MISR height distributions were produced for each observed plume in Kamchatka (see Supplemental Material). Comparing these profiles highlights the distinct dispersion characteristics of remobilized ash vs. erupted plumes (Fig. 2). Traditional eruption reports identify multiple instances when plumes were produced by re-suspension of previously deposited volcanic material (Global Volcanism Program, 2015; 2016). In a number of additional cases, these plumes occurred during registered periods of quiescence at the volcanoes from which they originated (KVERT, 2016a; 2016b), suggesting the events are not generated by primary volcanic activity. However, not all remobilized ash plumes identified here are classified as such by traditional reports, particularly where traditional observations are sporadic or monitoring relies on alternative (non-MISR) space-borne remote sensing observations. Of the 19 MISR-identified remobilized plumes, the majority (16) occurred at Shiveluch volcano (56.65°N, 161.36°E). Single observations were registered at: Karymsky (54.05°N, 159.44°E) and Kliuchevskoi (56.06°N, 160.64°E), and two events at Kizimen (55.13°N, 160.32°E).

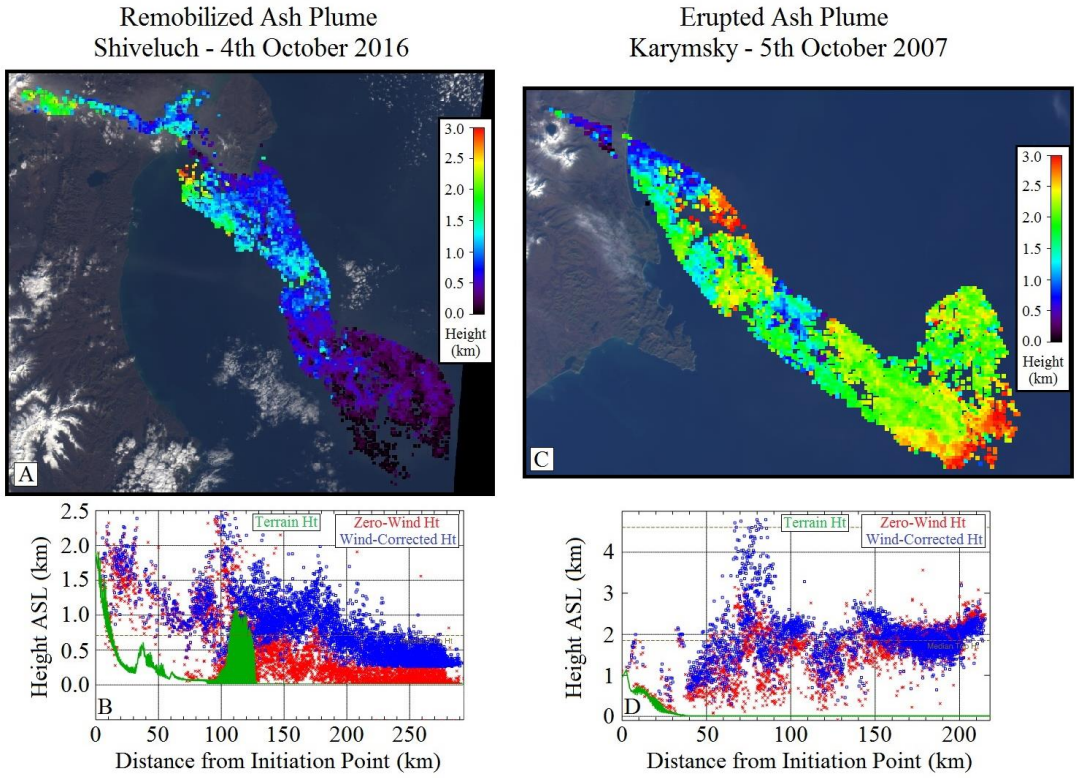

Figure 2 – MISR red-band stereo height retrieval maps (top) and height distributions as a function of distance from the vent (bottom), for a remobilized ash plume at Shiveluch (left - Terra Orbit: 89366; Path: 98; MISR Blocks: 45-47) and an erupted ash plume from Karymsky volcano (right - Terra Orbit: 41469; Path: 97; MISR Blocks: 46-47). MISR stereo-derived height distributions assuming no wind correction are marked in red, whereas blue points show heights derived with the parallax corrected for plume motion. Heights are all reported above the geoid; green points indicate the surface elevation in the lower plots. Note that the horizontal and vertical scales differ for plots (B) and (D), but the color bars used in (A) and (C) are identical.

The documented (Global Volcanism Program, 2016) Shiveluch remobilized ash plume (Fig. 2a) occurred on October 4, 2016. The MISR plume height distribution indicates the suspended particles were confined to the boundary layer (<1.5 km above terrain height) and exhibit a general downward trajectory (Fig. 2b). In contrast, the eruptive plume from Karymsky (Fig. 2d) displays a measure of buoyancy despite being emitted at low altitude. Separation between the plume base and surface terrain is clearly visible in the erupted plume (Fig. 2d).

Remobilized ash plumes consistently display characteristics similar to density flows (see Supplemental Material). Wind speeds, and corresponding particle lofting, tend to respond to changes in slope angle, downslope obstacles and changes in surface type, similar to the dispersion dynamics of pyroclastic density currents (Dufek et al., 2015). Ash remobilization is primarily driven by meteorological forcing (i.e., high near-surface wind speed; low relative humidity) and therefore is relatively independent of eruptive activity at the volcano of origin. Reported

remobilized ash events in Iceland and at Katmai (Alaska) were found to display similar dispersion characteristics to Kamchatka events (see Supplemental Material).

3.2. Particle characteristics

The MISR RA was used to investigate the particle microphysical properties of both erupted volcanic plumes and re-suspended ash (Fig. 3). Detailed MISR RA analysis in the current study is limited to over-ocean regions. Due to their proximity to the coast and relatively simple local topography, plumes generated by Shiveluch and Karymsky dominate results presented here. Based on these retrievals, remobilized plumes contain a large fraction of non-spherical particles (Fig. 3b) with minimal absorption (Fig. 3c), and show minimal variation across the plume length (Supplemental Material gives the results for all cases). In contrast, erupted plumes generally contain a higher fraction of small spherical particles (Fig. 3e) and relatively more absorption (Fig. 3f). Erupted plumes also exhibit greater lateral dispersion from the plume core than remobilized plumes, as the fringes of the latter are more distinctly defined in the RA output (Fig 3). The edges of erupted plumes have lower AOD than the plume core, but still indicate higher absorption (Fig. 3f) compared to remobilized ash plumes of equivalent size. The particle properties identified in erupted plumes vary depending upon eruption magnitude and magma composition (e.g., Scollo et al., 2012). Variations in volatile content between eruptions generate deviations in the RA-retrieved components (see Supplemental Material). In contrast, remobilized events are less sensitive to magma composition and as such, display minimal shifts in particle properties over time. The retrievals indicate that remobilized plumes are consistently dominated by large (~ 1.28 μm), non-absorbing (SSA > 0.99) particles.

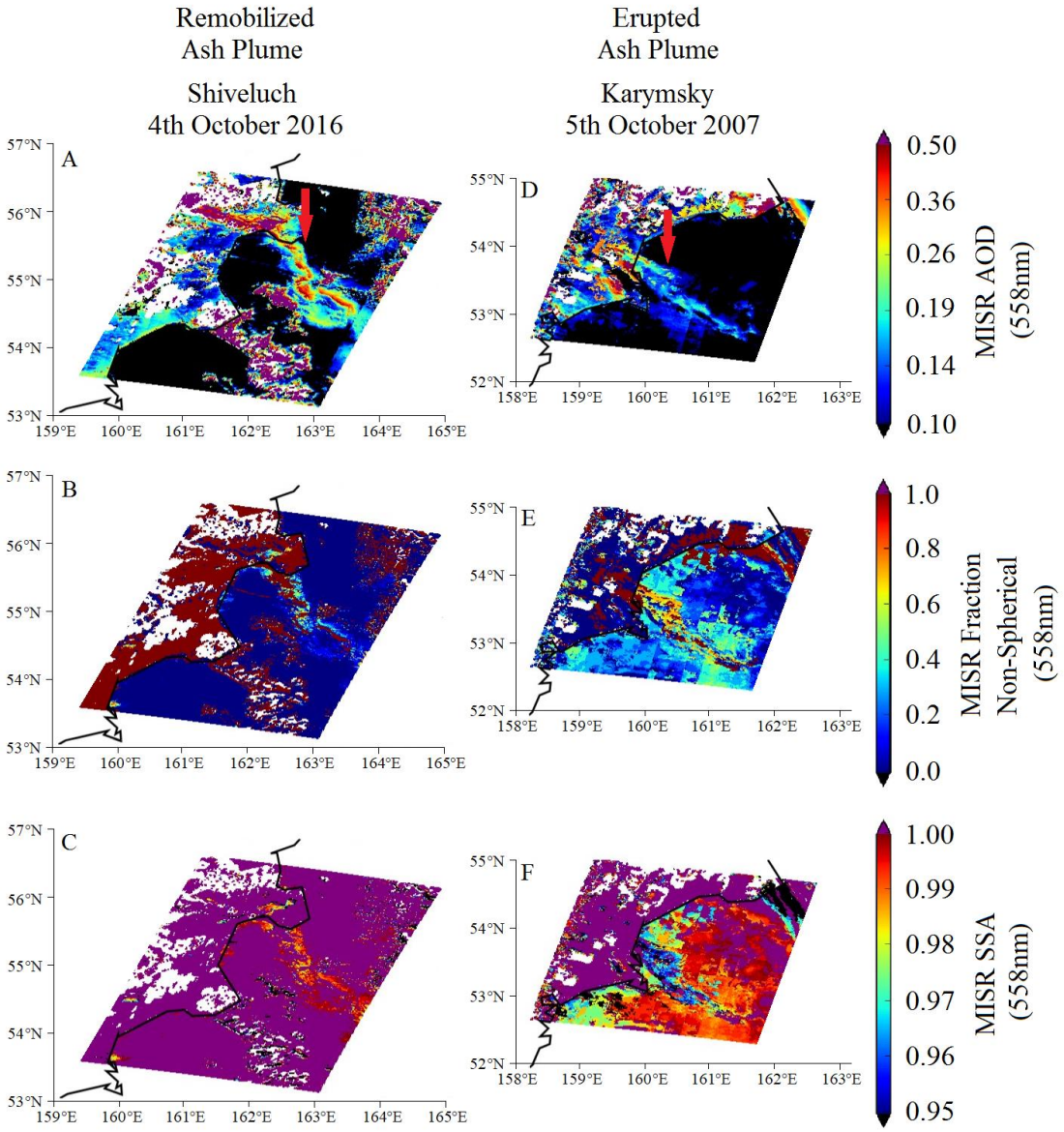

Figure 3 – MISR Research Algorithm particle properties for two volcanic plumes. Maps in the left column were derived from a remobilized ash plume generated at Shiveluch on October 4, 2016 (Terra Orbit: 89366; Path: 98; MISR Blocks: 45-47). The right column shows corresponding results for an erupted plume from Karymsky volcano on October 5, 2007 (Terra Orbit: 41469; Path: 97; MISR Blocks: 46-47). Three MISR-retrieved plume characteristics are included: Aerosol Optical Depth (AOD) - representing column aerosol amount; AOD fraction of non-spherical particles; and SSA, representing levels of light absorption by plume particles, with lower values indicating greater particle absorption. Red arrows indicate plume locations in Panels A and D.

Analysis of dominant mixtures retrieved using the 774-mixture RA climatology reveal that remobilized plumes are dominated by a single mixture: "mixture 14," characterized by large

(~1.28 μm) spherical non-absorbing particles with minimal (~5%) quantities of small spherical absorbing particles and medium, non-spherical grains (~5%). This mixture constitutes >84% of retrieved mixtures in all remobilized ash plumes analyzed (Fig. 4). In contrast, although erupted plumes from both Karymsky and Shiveluch contained this component (see Supplemental Material), it did not dominate the retrievals (three quarters of plumes displayed <45%). Eruptive plumes can also contain high proportions of large particles with minimal absorption and angularity, depending upon individual eruption characteristics. Due to similarities in the particle properties of essentially all observed remobilized ash plumes and *some* eruptive events, the MINX plume height profiles provide a more consistent method for distinguishing remobilized ash and eruptive volcanic plumes.

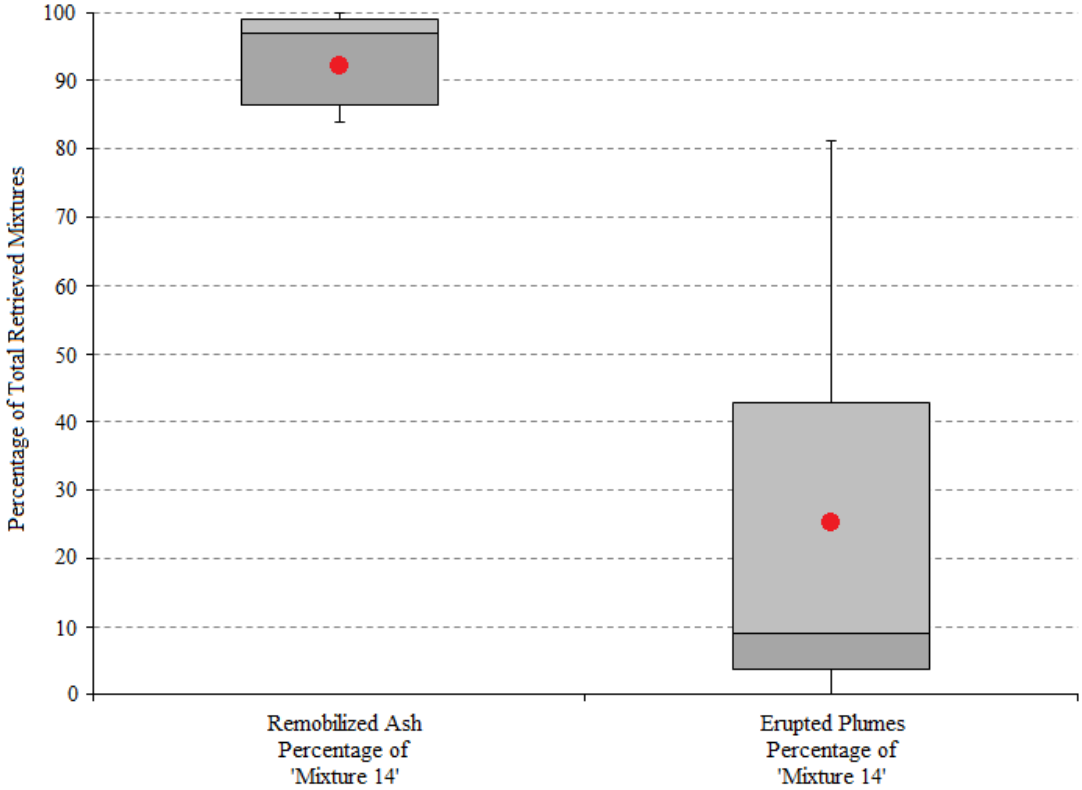

Figure 4 – Box plots showing the proportion of the dominant remobilized mixture ('Mixture 14'), for 19 remobilized events and 20 eruptive plumes imaged in Kamchatka, based on MISR RA retrievals run with the 774-mixture aerosol-type climatology.

4. Tracking particle dispersion

Individual remobilized ash plumes were investigated to determine if patterns of dispersion might reflect details of their transport dynamics. The MISR-generated height distributions allow us to assess the concentration and altitude of particles to some extent (see Section 2.1), and to compare these with the underlying geography of the area.

A large plume was observed at Kizimen volcano on January 1, 2011, following the resurgence of explosive activity on December 11, 2010. However, no direct observations were made at Kizimen during this period. Kizimen is located within an inland mountain range, resulting in greater susceptibility to terrain influence on low-altitude plumes. Initial identification resulted from a stark variation in surface reflectance observed in MODIS images from December 30, 2010 and January 1, 2011. The MODIS imagery cannot distinguish previously deposited from low-altitude suspended particulates, so the status of the event could not be ascertained from these data alone. MISR maps of suspended particle elevation reveal key information regarding plume dispersion dynamics. This plume was analyzed in four segments due to apparent variations in wind direction: the inland valley (IV) region and three distinct ocean entries (OE) (Fig. 5). Each profile is color-coded based on the initiation point of the plume retrieval for that segment. In the IV retrieval (purple), particles concentrated below 2 km ASL, ~1 km above the terrain. A mountain range running parallel to the coast, with peaks exceeding the maximum plume altitude (2.5 km), confined the particles within the adjacent inland valley. The control of particle dispersion by the local terrain categorizes this plume, and similar events, as topographically restricted hazards. As such, the risks associated with these events could be mapped for predictive purposes, using techniques similar to those applied to map lahars, landslides, and other topographically defined hazards.

Visual inspection of each OE region with a nadir-viewing instrument such as MODIS indicates lateral dispersion. However, MISR profiles provide additional constraints on the vertical distribution of particles during transport. In each OE profile (green, blue, and orange), plume uplift is observed over ocean, with a peak in particle altitude occurring ~20 km from the coast. OE1 (green) displays the largest vertical variation, showing an increase from the average plume height (0.5 km) up to ~1.5 km. OE2 (blue) and OE3 (orange) both display altitude increases of ~0.5 km above their respective average plume heights. Differences in the valley widths of each ocean entry, and the distances from the narrowest valley point to the ocean, are likely to have influenced the respective concentrations and vertical dispersion. OE1 is characterized by the widest ocean entry. Correspondingly, OE1 produced the most diffuse outlet due to lateral dispersion, with only 23% of the visible plume area containing sufficient AOD for MINX retrievals, compared to 46% and 50% for OE2 and OE3, respectively. The restriction of particle

release to valley regions would produce a strong pressure gradient, causing a corresponding increase in wind speed. MISR-retrieved wind speeds (Fig. 5) indicate that wind speed increased from < 4 m/sec to 18 m/sec, 11 m/sec and 16 m/sec for OE1 to OE3, respectively, following transition over the ocean in each analysis.

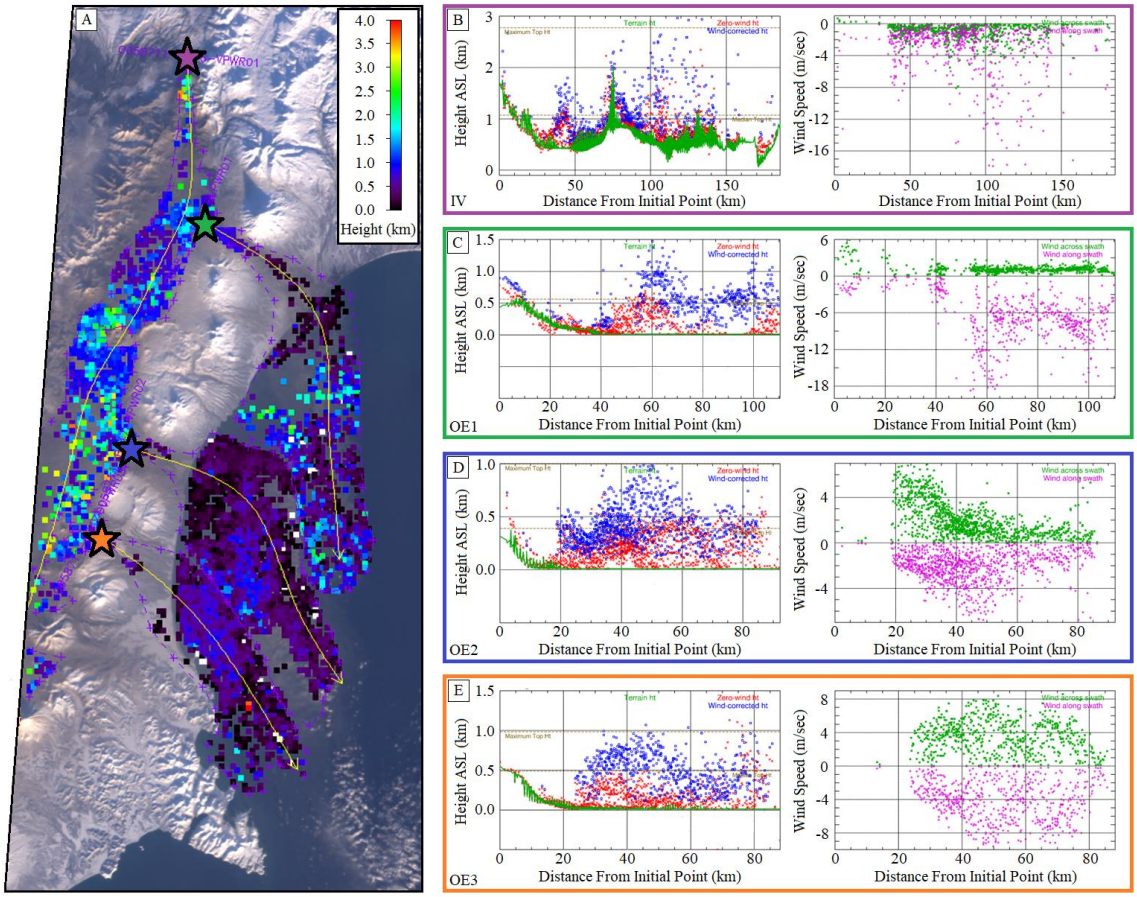

Figure 5 – (A) MISR red-band stereo height retrieval map. (B-E) height profiles (Column 2) and wind speed (Column 3), as functions of distance, of a remobilized ash plume produced at Kizimen volcano on January 1, 2011 (Terra Orbit: 58711; Path: 97; MISR Blocks: 46-48). Plume elevation map (A); yellow lines denote user-defined wind direction for each plume. In the adjacent plots, MISR stereo-derived height distributions assuming no wind correction are marked in red; wind corrected points are shown in blue. Green points indicate the surface elevation above the geoid. Colored borders correspond to IV and OE plumes (see text). Note that the horizontal and vertical scales vary from panel to panel (B-E).

The local topography also appears to significantly influence the dispersion of remobilized ash from Shiveluch (see Supplemental Material). Remobilized plumes predominantly disperse to the east, due to the horseshoe configuration of the Shiveluch caldera, breached to the southeast. Activity at Shiveluch is characterized by lava dome growth and collapses, with tephra layers deposited within the caldera (Global Volcanism Program, 2013). When strong winds occur,

dispersion of deposited particles is impeded to the north, south and west by the caldera rim. The easterly-dispersing remobilized plumes follow similar paths, transiting to the coast in the Kamchatka River valley over the settlement of Ust-Kamchatsk (56.22°N, 162.48°E).

5. Discussion and Conclusions

This work demonstrates that the profiling capabilities of MISR global, space-based multi-angle observations can be used to distinguish remobilized ash events from ongoing eruptive activity. Remobilized ash is generated under similar meteorological conditions, irrespective of the volcano of origin with particles confined in the boundary layer (typically <1.5 km). Although the results here focus on the Kamchatka region, the plume height technique can be applied globally, limited primarily by the MISR observation frequency (~2-8 days depending on latitude). Local topography has a strong influence on the dispersion of these low-altitude, limited-buoyancy plumes, as expected. Therefore, events occurring inland are more likely to pose a hazard to downslope populations than those occurring near the coastline, where particles are rapidly dispersed over ocean.

In-depth analysis of particle microphysical properties, based on MISR RA retrievals, indicates relative uniformity regardless of particle source, both within individual remobilized ash plumes and between discrete events. This consistency is in contrast to erupted plumes, which vary, both across plume length and between events. Whilst the current RA particle optical property options are not optimized for volcanic plumes and there is limited capability to distinguish among sub-groups of large-sized particles, clear qualitative differences can be seen between remobilized ash and erupted plume particles.

To distinguish remobilized ash from erupted volcanic plumes imaged by MISR, plume height distributions can be pre-screened to identify those showing limited buoyancy and having particles confined within the boundary layer. Uniform, particle property retrievals, comprised primarily of large spherical non-absorbing particles (mixture ‘14’), would further support identification as remobilized-ash. However, care must be taken when applying the particle microphysical property distinction alone, as eruptions with minimal volatiles can generate similar RA signatures to remobilized plumes.

Separating erupted from remobilized plumes will improve eruption frequency calculation, prevent aliasing volcanic plume studies with those generated by secondary processes, and could help with secondary volcanic hazard identification and modeling. As this is a satellite remote-sensing technique, it can be applied globally, even in remote regions where suborbital monitoring is lacking.

Acknowledgements

The work of V.J.B. Flower is supported by an appointment to the NASA Postdoctoral Program at the NASA Goddard Space Flight Center, administered by Universities Space Research Association under contract with NASA. The work of R. Kahn is supported in part by NASA's Climate and Radiation Research and Analysis Program under H. Maring, NASA's Atmospheric Composition Program under R. Eckman, and the NASA Earth Observing System's MISR project. We thank James Limbacher for his assistance in the installation of the MISR 774-mixture Research Aerosol algorithm and his ongoing technical support.

MISR data is freely available from NASA Langley Research Center's Atmospheric Science Data Center (ASDC). Plume height and basic particle properties can be derived with the MINX software package available from Open Channel Foundation (http://www.openchannelsoftware.com/projects/MINX).

6. References

Diner, D. J., Beckert, J. C., Reilly, T. H., Bruegge, C. J., Conel, J. E., Kahn, R. A., Martonchik, J.V., Ackerman, T.P., Davies, R., Gerstl, S.A. & Gordon, H. R. (1998). Multi-angle Imaging SpectroRadiometer (MISR) instrument description and experiment overview. IEEE Transactions on Geoscience and Remote Sensing, 36(4), 1072-1087.

Dufek, J., Ongaro, T. E., & Roche, O. (2015). Pyroclastic density currents: Processes and models. *The encyclopedia of volcanoes*, 631-648. DOI:10.1016/B978-0-12-385938-9.00035-3

Flower, V. J., & Kahn, R. A. (2017). Assessing the altitude and dispersion of volcanic plumes using MISR multi-angle imaging from space: Sixteen years of volcanic activity in the Kamchatka Peninsula, Russia. *Journal of Volcanology and Geothermal Research*.

Global Volcanism Program, 2013. Sheveluch (300270) *in* Volcanoes of the World, v.4.6.2. Venzke, E (ed.). Smithsonian Institution. Downloaded 28 Sep 2017. (http://volcano.si.edu/gvp_votw.cfm?vn=300270). DOI:10.5479/si.GVP.VOTW4-2013.

Global Volcanism Program, 2015. Report on Sheveluch (Russia). In: Sennert, S K (ed.), Weekly Volcanic Activity Report, 16 September-22 September 2015. Smithsonian Institution and US Geological Survey.

Global Volcanism Program, 2016. Report on Sheveluch (Russia). In: Sennert, S K (ed.), Weekly Volcanic Activity Report, 5 October-11 October 2016. Smithsonian Institution and US Geological Survey.

Kahn, R.A., P. Banerjee, and D. McDonald, 2001. The Sensitivity of Multiangle Imaging to Natural Mixtures of Aerosols Over Ocean, *J. Geophys. Res.106*, 18219-18238.

Kahn, R. A., Li, W. H., Moroney, C., Diner, D. J., Martonchik, J. V., & Fishbein, E. (2007). Aerosol source plume physical characteristics from space-based multiangle imaging. *Journal of Geophysical Research: Atmospheres*, *112*(D11).

Kahn, R. A., & Limbacher, J. (2012). Eyjafjallajökull volcano plume particle-type characterization from space-based multi-angle imaging. *Atmos. Chem. Phys*, *12*(20), 9459-9477.

Kahn, R. A., and B. J. Gaitley, (2015). An analysis of global aerosol type as retrieved by MISR. *J. Geophys. Res. Atmos. 120*, doi:10.1002/2015JD023322Moroney, C., Davies, R., & Muller, J. P. (2002). Operational retrieval of cloud-top heights using MISR data. IEEE Transactions on Geoscience and Remote Sensing, 40(7), 1532-1540.

Kalashnikova, O. V., Kahn, R., Sokolik, I. N., & Li, W. H. (2005). Ability of multiangle remote sensing observations to identify and distinguish mineral dust types: Optical models and retrievals of optically thick plumes. *Journal of Geophysical Research: Atmospheres*, *110*(D18).

Kalashnikova, O. V., & Kahn, R. (2006). Ability of multiangle remote sensing observations to identify and distinguish mineral dust types: 2. Sensitivity over dark water. *Journal of Geophysical Research: Atmospheres*, *111*(D11).

Kalashnikova, O. V., & Kahn, R. A. (2008). Mineral dust plume evolution over the Atlantic from MISR and MODIS aerosol retrievals. *Journal of Geophysical Research: Atmospheres*, *113*(D24).

KVERT, (2016a). VONA/KVERT Daily Report, July 25, 2016. Institute of Volcanology and Seismology FEB RAS. URL: http://www.kscnet.ru/ivs/kvert/van/?n=2016-07-25.

KVERT. (2016b). VONA/KVERT Daily Report, September 20, 2016. Institute of Volcanology and Seismology FEB RAS. URL: http://www.kscnet.ru/ivs/kvert/van/?n=2016-09-20.

Limbacher, J. A., & Kahn, R. A. (2014). MISR research-aerosol-algorithm refinements for dark water retrievals. *Atmospheric Measurement Techniques*, *7*(11), 3989-4007.

Limbacher, J. A., & Kahn, R. A. (2017). Updated MISR dark water research aerosol retrieval algorithm–Part 1: Coupled 1.1 km ocean surface chlorophyll a retrievals with empirical calibration corrections. *Atmospheric Measurement Techniques*, *10*(4), 1539-1555.

Muller, J. P., Mandanayake, A., Moroney, C., Davies, R., Diner, D. J., & Paradise, S. (2002). MISR stereoscopic image matchers: Techniques and results. IEEE Transactions on Geoscience and Remote Sensing, 40(7), 1547-1559.

Nelson, D. L., Chen, Y., Kahn, R. A., Diner, D. J., & Mazzoni, D. (2008). Example applications of the MISR INteractive eXplorer (MINX) software tool to wildfire smoke plume analyses. In Proc. SPIE (Vol. 7089, pp. 708909-1)

Nelson, D. L., Garay, M. J., Kahn, R. A., & Dunst, B. A. (2013). Stereoscopic height and wind retrievals for aerosol plumes with the MISR INteractive eXplorer (MINX). *Remote Sensing*, *5*(9), 4593-4628.

Scollo, S., Folch, A., Coltelli, M., & Realmuto, V. J. (2010). Three-dimensional volcanic aerosol dispersal: A comparison between Multiangle Imaging Spectroradiometer (MISR) data and numerical simulations. *Journal of Geophysical Research: Atmospheres*, *115*(D24).

Scollo, S. R.A. Kahn, D.L. Nelson, M. Coltelli, D.J. Diner, M.J. Garay, and V.J. Realmuto, 2012. MISR observations of Etna volcanic plumes. *J. Geophys. Res*. *117*, D06210, doi:10.1029/2011JD016625.

Sigurdsson, H., Houghton, B., McNutt, S., Rymer, H., & Stix, J. (Eds.). (2015). *The encyclopedia of volcanoes*. Elsevier.